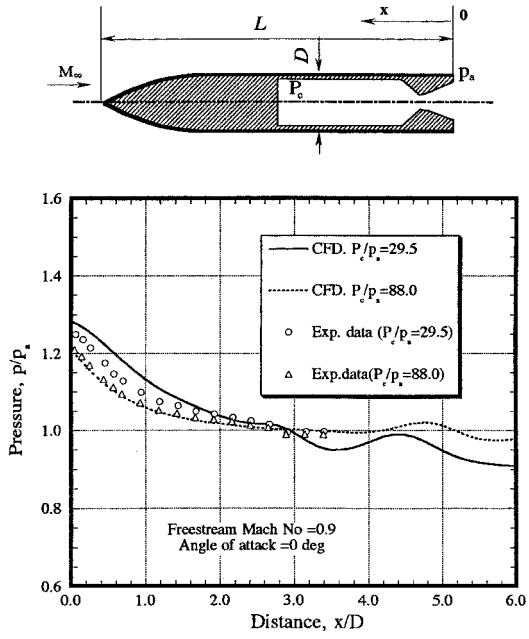

Fig. 4 Comparison of CFD results and wind-tunnel data: tangent-ogive cone cylinder model with plume.

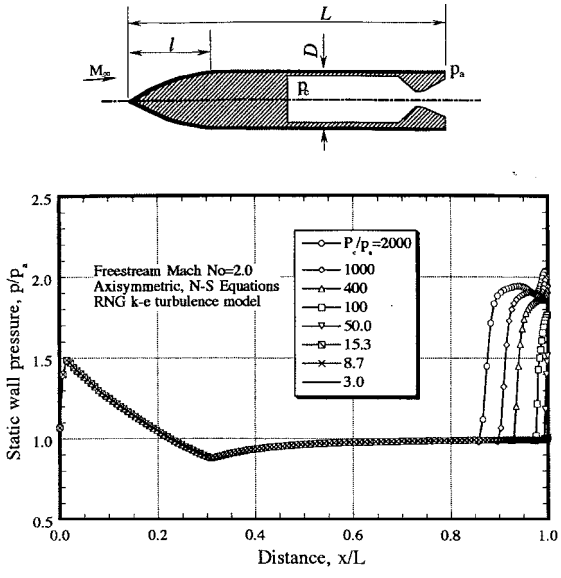

Fig. 5 Static pressure distributions along the body surface ($M_0 = 2.0$): tangent-ogive cone cylinder model with plume.

pressure ratio, the plume-induced shock wave moves upstream. Therefore, it may be reasonable to conclude that an increase in the plume pressure ratio has a similar effect to that of a decrease in the freestream Mach number. Note that there exists a large region of separation at the foot of the plume-induced shock on the body.

Conclusions

The conclusions from these analyses are as follows: Several features of plume flow and its interference effects on aft-mounted control surfaces can be clearly identified by CFD analysis. Plume pressure ratio has a significant effect on the plume in reference. For a given plume pressure ratio, an increase in Mach number resulted in an increase in shock strength and rearward motion of the shock on the tail fin.

References

[1]Dryer, N., and North, W. J., "Preliminary Analysis of the Effect of Flow Separation Due to Rocket Jet Pluming on Aircraft Dynamic Stability During Atmospheric Exit," NASA Memo 4-22-59E, 1959.

[2]Alpinieri, T. C., Jr., and Adams, R. H., "Flow Separation due to Jet Pluming," *AIAA Journal*, Vol. 4, No. 10, 1966, pp. 1865, 1866.

[3]McGhee, R. J., "Jet-Plume-Induced Flow Separation on a Lifting Entry Body at Mach Numbers from 4.00 to 6.00," NASA TM X-1997, April 1970.

[4]Klineberg, J., Kubota, T., and Lees, L., "Theory of Exhaust-Plume/Bounday-Layer Interactions at Supersonic Speeds," *AIAA Journal*, Vol. 10, No. 5, 1972, pp. 581–588.

[5]Boger, R. C., Rosenbaum, H., and Reeves, B. L., "Flowfield Interactions Induced by Underexpanded Exhaust Plumes," *AIAA Journal*, Vol. 10, No. 3, 1972, pp. 300–306.

[6]Burt, J. R., Jr., "An Investigation of the Effectiveness of Several Devices in Simulating a Rocket Plume at Free Stream Mach Numbers of 0.9 to 1.2," U.S. Army Missile Command, RD-TR-71-22, Redstone Arsenal, AL, Sept. 1971.

R. M. Cummings
Associate Editor

Implementation of an Aerodynamic Toolbox in a Reentry Flight Simulator

A. Guidi,* Q. P. Chu,† J. A. Mulder,‡ and J. Buursink§
Delft University of Technology,
2629 HS Delft, The Netherlands

Nomenclature

C_A	=	axial-force coefficient
C_{Ab}	=	axial-force coefficient of the base pressure
C_f	=	friction coefficient
C_M	=	moment coefficient
C_N	=	normal force coefficient
C_{Nb}	=	normal force coefficient of the base pressure
C_p	=	pressure coefficient
C_{pb}	=	pressure coefficient of the base pressure
$C_{p\,max}$	=	pressure coefficient in stagnation point
c	=	reference length, m
F	=	force, N
F_x	=	force in x direction, N
F_y	=	force in y direction, N
i	=	unit vector in x direction
j	=	unit vector in y direction
L	=	reference length, m
M	=	Mach number
M	=	moment, Nm
n	=	vector perpendicular to the surface
$P_{stagnation\ max}$	=	maximum stagnation point pressure, Pa
p	=	pressure, Pa
p_{stag}	=	stagnation point pressure, Pa
p_∞	=	freestream pressure, Pa
R, r	=	radius, m
R_B	=	base radius, m
R_N	=	nose radius, m

Received 10 October 2001; revision received 10 April 2002; accepted for publication 23 September 2002.

*Aerospace Engineer; currently Aerospace Engineer, University of Naples "Federico II," Via A. D'Isernia, 59, 80122 Naples, Italy; oceanomare@inwind.it. Member AIAA.

†Assistant Professor, Control and Simulation Division, Delft Aerospace, Kluyverweg, 1. Senior Member AIAA.

‡Professor, Chairman of the Control and Simulation Division, Delft Aerospace, Kluyverweg, 1. Senior Member AIAA.

§Research Assistant, Delft Aerospace, Kluyverweg, 1. Member AIAA.

S = aerodynamic reference area, m^2
U_∞ = freestream velocity in x direction, m/s
θ = local deflection angle (Euler angle), deg
ρ_∞ = freestream air density, kg/m^3
σ_N = normal momentum accommodation
σ_T = tangential momentum accommodation

Introduction

THIS work was started during the stability analysis of the preliminary design for the Delft Aerospace Reentry Test demonstrator (DART). DART is a small axial-symmetric reentry vehicle that Delft Aerospace is proposing to build together with other European partners. Two concept shapes are under study, REVolution and Volna.[1]

In this design phase a strong interaction between different disciplines is demanded for an effective design. One crucial factor among the several fields of a preliminary design of an aircraft is the aerodynamics of the vehicle body.[2] The estimation and measurement of the aerodynamic characteristics of the vehicle give its representation in the flight simulator. Aerodynamic analysis is usually performed with computational fluid dynamics software, which is mostly concerned with the solution of the system of partial differential equations of Navier–Stokes. These kinds of calculations are rather complex and require a large amount of computer power. However, another necessity during the preliminary phase is to have a relatively simple way of evaluation for different solutions of the design. This is necessary so that a quick and iterative process will lead to a final design that meets all of the requirements and objectives. The objective is to implement a simple and as complete as possible aerodynamic toolbox for a reentry flight simulator. The aerodynamic regimes implemented in the toolbox are hypersonic free molecular flow, hypersonic transitional, and hypersonic continuum, all with the influence of viscosity.

Hypersonic Free Molecular Flow

Flow regimes differ depending on different levels of rarefaction of the atmosphere, which can be represented by the mean free path between molecules. For the free molecular flow the kinematics model of interaction particle surface postulated by Maxwell is used. An inclination method derived from this theory[3] is implemented. The following equations give the values of the pressure and friction coefficients:

$$C_p = 2(2 - \sigma_N)\sin^2\theta, \qquad C_f = 2\sigma_T \cos\theta \sin\theta \tag{1}$$

where σ_N and σ_T are

$$\sigma_N = \frac{P_i - P_r}{P_i - P_w}, \qquad \sigma_T = \frac{\tau_i - \tau_r}{\tau_i} \tag{2}$$

From the pressure and friction coefficients once projected on the body frame, the axial coefficient C_A, the normal coefficient C_N, and the moment coefficient C_M can be calculated:

$$\frac{F}{q_\infty S} = \sum_{i=1}^{m} \left\{ C_{P_i}(-n_i) + C_{\tau_i}[\hat{n}_i \times (\hat{V}_\infty \times \hat{n}_i)] \right\} \mathrm{d}s$$

$$\frac{M}{q_\infty Sc} = \sum_{i=1}^{m} \left(r_i \times \left\{ C_{p_i}(-\hat{n}_i) + C_{\tau_i}[\hat{n}_i \times (V_\infty \times \hat{n}_i)] \right\} \right) \mathrm{d}s \tag{3}$$

Force and moment have then to be integrated on the surface of the body in order to obtain the value of the total force and moment acting on the body. This integration for the free molecular flow will be made through a panel method explained in the following paragraph.

Hypersonic Transitional Flow

The two different flow regimes must be linked so that they cover any specific flight condition. A bridge function is needed. The dominance of one flow on the other is simply dependent on the logarithmic of the Knudsen number. Defining M_{rar} the weight of the rarefied flow, $1 - M_{\mathrm{rar}}$ will be the weight of the continuum. According to Regan,[4]

$$M_{\mathrm{rar}} = a \cdot \mathrm{erf}[b \cdot \log(Kn) + c] + a \tag{4}$$

where $a = 0.5$, $b = 0.30709257318569$, and $c = 0.80628539465167$ and are obtained statistically.

Hypersonic Continuum Flow

For the continuum flow the modified Newtonian law

$$C_p = C_{p\max} \sin^2\theta \tag{5}$$

was integrated for the biconical blunted cone shape. The modified Newtonian law is a so-called surface inclination method. It is a nonlinear extension of the result that was obtained for inviscid flow over body in supersonic and subsonic flow where simply from the inclination of the surface it was possible to determine the pressure. $C_{p\max}$ equals exactly the C_p in the stagnation point behind a normal shock wave. The total pressure behind a normal shock wave, at the freestream Mach number, can be calculated using the exact shock-wave theory.[5]

The force coefficients for a sphere and for a cone need to be determined. For simplicity, an expression for the forces in a body-fixed coordinate system is developed. The axial force and the normal force are given by the following formulas[6]:

$$C_A = \frac{1}{\left(\frac{1}{2}\rho_\infty U_\infty^2\right)\left(\pi R_b^2\right)} \oiint_S (p - p_\infty)(\hat{n}\,\mathrm{d}S) \cdot \hat{i} \tag{6}$$

$$C_N = \frac{1}{\left(\frac{1}{2}\rho_\infty U_\infty^2\right)\left(\pi R_b^2\right)} \oiint_S (p - p_\infty)(\hat{n}\,\mathrm{d}S) \cdot (-\hat{j}) \tag{7}$$

where the integral has to be calculated for the three different parts of the blunt biconical shape. For the continuum flow a direct numerical integration was used.

Finally an approximation of the base pressure can be calculated using the Gaubeaud formula:

$$C_{p_b} = \frac{2}{\gamma M_\infty^2}\left\{ \left(\frac{2}{\gamma+1}\right)^{1.4} \left(\frac{1}{M_\infty}\right)^{2.8} \left[\frac{2\gamma M_\infty^2 - (\gamma - 1)}{\gamma + 1}\right] - 1 \right\} \tag{8}$$

From the base pressure coefficient the C_{Nb} and the C_{Ab} can be calculated with

$$C_{N_b} = C_{p_b}\sin\alpha, \qquad C_{A_b} = -C_{p_b}\cos\alpha \tag{9}$$

For the C_M the moment around the sphere-cone apex was calculated through the value of the axial and normal component of the forces. The final value of C_M is obtained as the sum of all of the contributions for the single part of the multibody.

Viscous Influence in the Hypersonic Continuum Flow

The viscosity plays a relevant role in the hypersonic regime. The viscous effect generates two forces acting on the body. One is tangential to the surface of the body and comes mainly from a phenomenon of shear stresses in the boundary layer. The second is normal to the shape and is caused mainly by the presence of the boundary layer itself; in hypersonic theory this last phenomenology is often called viscous interaction. As already mentioned, this will be a basic piece of work; therefore, an engineering approach was used.

The tangential force was implemented by calculating the friction coefficient with an engineering approximation called Reference Temperature method. This method accounts for compressible effect using incompressible method, and it is based on the assumption of a dependency of the value of C_f from a reference temperature somewhere inside the boundary layer. Without going deep into the explanation of this method,[3,5] the formulas implemented for the laminar and turbulent boundary layer are, respectively,

$$C_f = \frac{0.664}{\sqrt{Re_x}(T'/T_\infty)^{(1-\omega)/2}}, \qquad C_f = \frac{0.0592}{\sqrt[5]{Re_x}\cdot(T'/T_\infty)^{(1-\omega)/5}} \tag{10}$$

In both cases the T' is named total temperature and is a function of Mach and T_∞ in the undisturbed flow:

$$T'/T_\infty = 1 + [(\gamma - 1)/2] \cdot M_\infty^2 \tag{11}$$

Both these formulas are for a flat plate. To apply the preceding results to cones, simply multiply the right-hand side of the equation by the Mangler fraction, $\sqrt{3}$.

In the study of the viscosity, an important phenomenon is involved: the transition between laminar and turbulent flow. For the accurate prediction of skin friction, the knowledge of the transitional Reynolds number is critical. However no theory exists for accurate prediction of Re_T . Any knowledge concerning it comes from experimental data.[7] For the transition between the two different regimes, turbulent and laminar, an engineering approximation is used. In this approximation the transition is related to the value of the Reynolds number.[3] The value of the Re_T is assumed to be function of the Mach number through

$$\log(Re_T) = 6.421 \exp\left(1.209 \times 10^{-4} \cdot M_e^{2.641}\right) \tag{12}$$

$$Re_T = \rho_e V_e x_T / \mu_e \tag{13}$$

Once the value of Re for transition is known, it is easy to determine the distance xt where transition occurs.

The normal force, estimated with the engineering method related to experimental data, is applied. Within the viscous interaction two other phenomena can be identified, and, as is common in aerodynamics, they can be related to a similarity parameter: the viscous interaction parameter $\bar{\chi}$:

$$\bar{\chi} = \frac{M_\infty^3}{\sqrt{Re}} \sqrt{\frac{\rho_w \mu_w}{\rho_e \mu_e}} \tag{14}$$

The $\bar{\chi}$ is used to determine the transition between the two different kinds of interaction: "strong" and "weak." A large value of $\bar{\chi}$ corresponds to the strong interaction and vice versa. The value associated with transition is for practical purposes assumed to be three. Also, it is directly related to the value of the pressure through

$$P/P_\infty = 1 + 0.5\bar{\chi}, \qquad P/P_\infty = 1 + 0.078\bar{\chi} \tag{15}$$

respectively, in the case of strong and weak interaction.

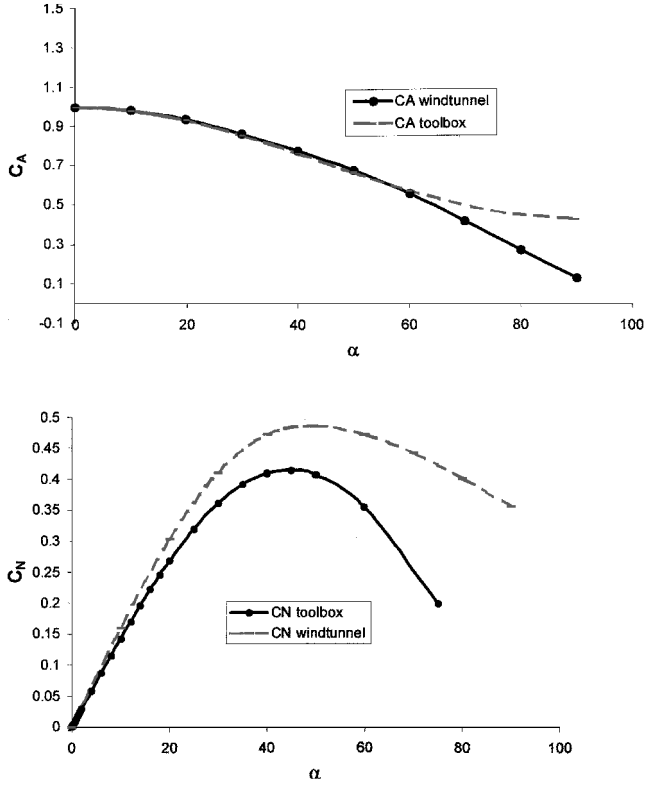

Fig. 1 C_A **and** C_N **from the toolbox and from wind-tunnel data in continuum flow for the IRDT vehicle.**

The discussed viscous interaction happens in case of a laminar boundary layer. In case of a turbulent boundary layer, the same adjustment would have to be made. However, most viscous interaction theory is based on laminar flow because it occurs at large Mach numbers and small Reynolds numbers, and this condition promotes laminar boundary layer.

Integration of the Coefficients with the Panel Method

All of the methods just discussed are local methods that need to be integrated over the shape of the body. Numerical integration is feasible for a relative simple shape, but can be difficult in the study of a complex structure. To maintain the toolbox as general as possible, for the free molecular integration the panels method is used. Basically the shape is discretized in the way of a classic finite element method, and then the pressure coefficients are applied to all of the panels, summed, and divided into the different components.

Validation

The validation of the toolbox was executed in two ways. First the output of the value of a single aerodynamic coefficient over a flat plate is calculated and compared with literature data,[7] and an error of less then 10% was obtained. Then most important validation was obtained implementing in the software the configuration characteristics of the Inflatable Reentry and Descent Technology (IRDT) a 45-deg blunted cone vehicle. IRDT was an ESA-DASA (German Aerospace Agency) mission and ESA furnished us wind-tunnel data of the vehicle that were used for comparison of the result obtained from the toolbox. In Figs. 1 and 2 this comparison is shown. The error in the axial coefficient and normal coefficient is increasing with the angle of attack. Particularly good results are obtained with the C_A in the continuum and rarefied flow, where the two curves match up to an angle of attack of around 50 deg for the continuum and for all values for the rarefied flow regime. In the case of C_N in continuum flow, the error increases significantly beyond a value of alpha of about 20 deg and up to 35 deg in the rarefied flow.

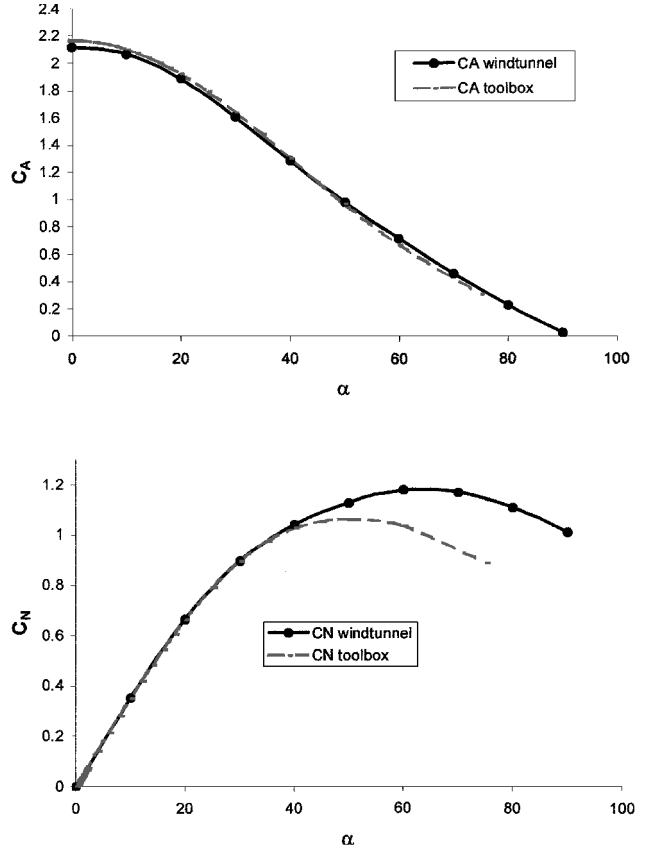

Fig. 2 C_A **and** C_N **from the toolbox and from wind-tunnel data in free molecular flow for the IRDT vehicle.**

Conclusions

The objective of this Note was to build a method in order to estimate the aerodynamic characteristics of an axial-symmetric vehicle during reentry. The method can be considered an engineering one and is particularly suitable for feasibility study and for the early design phase. The best way to use this method is to implement all of the equations in a software such as C++ or Matlab/Simulink.

References

[1]Buursink, J., and Van Baten, T. J., "DART—The Delft Aerospace Re-Entry Test Demonstrator," International Astronautical Federation, IAF Paper 00-V.4.07, Oct. 2000.

[2]Cook, M. V., *Flight Dynamic Principles*, Arnold, London, 1997.

[3]Zoby, E. V., Moss, J. N., and Sutton, K., "Approximate Convective-Heating Equations for Hypersonic Flows," *Journal of Spacecraft and Rockets*, Vol. 18, No. 1, 1981, pp. 64–70.

[4]Regan, Frank J., *Dynamics of Atmospheric Re-Entry*, AIAA, Washington, DC, 1994.

[5]Anderson, J. D., Jr., *Hypersonic and High Temperature Gas Dynamics*, AIAA, Reston, VA, 2000.

[6]Reshotko, Eli, "Boundary Layer Stability and Transition," *Annual Review of Fluid Mechanics*, Vol. 8, 1976, pp. 311–349.

[7]Bertin, J. J. , *Hypersonic Aerothermodynamics*, AIAA, Washington, DC, 1994.

M. S. Miller
Associate Editor

Radiating Fin Analysis Using an Extended Perturbation Series Solution Technique

D. K. Harris* and F. Simionescu†
Auburn University, Auburn, Alabama 36949

Introduction

RADIATOR panels typically used on space vehicles to reject waste thermal energy to space commonly have efficiencies under 100% as a result of temperature gradients along the radiating surface. For thermal designers this effect (fin efficiency η) is a frequently encountered design parameter during radiator panel sizing. The fin efficiency is defined as the actual heat radiated compared to the heat radiation possible if the entire fin existed at the base temperature T_b. Several complex fin analyses have been offered in the open literature, which give designers a good estimate on the radiator panel efficiency. Kuiken[1] demonstrated that fin methods work satisfactorily for nonlinear (radiating) problems but gave nongeneral results. Aziz and Na[2] used the initial value method to investigate convecting-radiating fins, whereas Nguyen and Aziz[3] used a finite difference approach to investigate different fin profile shapes. Karem and Eby[4] linearized the fourth-power radiation term to compute fin efficiencies for the case of a constant-flux environment radiating to a sink at a temperature of 0 K. Aziz[5] employed an extended perturbation series solution to the special case of no incident heat flux on the radiating fin. His solution technique proved successful, as more fully detailed in Aziz and Na,[6] and gave designers a simple 11-term series for η, which is expanded here to include the nonhomogeneous solution of radiating to a nonzero sink. The purpose of the current study was to provide designers with similar series expansions for cases where the radiator is exchanging energy with a sink at a temperature other than 0 K. The present study can be considered as a more general case because an environmental flux can be resolved as an equivalent sink temperature, as is often the method employed by designers in radiator panel sizing calculations. Finally, for the reader interested in a general discussion of fin efficiency they can refer to Kern and Kraus,[7] who give a phenomenal description of extended surface heat transfer.

Received 25 January 2002; revision received 18 May 2002; accepted for publication 14 August 2002.

*Assistant Professor, College of Engineering, 202 Ross Hall; dharris@eng.auburn.edu.

†Research Assistant, Department of Mechanical Engineering, 202 Ross Hall.

Analysis

Equation (1) describes the one-dimensional, steady-state, and radiating extended surface temperature profile along the length of any fin as a function of the distance from the base of the fin for the case of no incident flux. This equation is valid for any rectangular fin of constant thickness w, where x is the distance along the fin from the base, A_r is the area exposed to the heat sink at temperature T_s, k is the base material conductivity, A_c is the conductive cross-sectional area, L is the length of the fin, σ is the Stefan–Boltzmann constant, and ε is the emissivity of the fin.

$$\frac{kA_c}{L}\frac{\mathrm{d}^2T}{\mathrm{d}x^2} - \sigma A_r \varepsilon\left(T^4 - T_s^4\right) = 0 \tag{1}$$

By introducing the following nondimensional parameters, as developed by Aziz and Na,[6] a simpler form of Eq. (1) is rendered:

$$\Theta = \frac{T}{T_b}, \qquad \Theta_s = \frac{T}{T_s}, \qquad X = \frac{x}{L}, \qquad \zeta = \frac{2\sigma\varepsilon T_b^3 L^2}{kw}$$

For steady state with the boundary conditions describing a fin with uniform base temperature and an insulated tip, Eq. (1) becomes

$$\frac{\mathrm{d}^2\Theta}{\mathrm{d}X^2} - \zeta\left(\Theta^4 - \Theta_s^4\right) = 0 \tag{2}$$

with the transformed boundary conditions,

$$\Theta(0) = 1, \qquad \frac{\mathrm{d}\Theta(1)}{\mathrm{d}X} = 0$$

Solution Technique and Results

The approach taken in Ref. 5 was not to search for a particular solution to the nonlinear differential Eq. (2), but rather to describe the behavior of the solution. The technique used was to perform a regular perturbation series expansion on Θ, as shown in Eq. (3):

$$\Theta = \sum_{i=0}^{\infty} \zeta^i \Theta_i \tag{3}$$

In Ref. 5 (and many others) Θ_s was taken as 0 for simplicity. Next, by substituting Eq. (3) into Eq. (2) and combining like terms in powers of ζ yielded the infinite perturbation series solution. The first 11 terms were hand calculated by Aziz in Ref. 5, giving the

Table 1 SINDA model comparison with series solution; Eqs. (5) and (6)

		Sinda results		Series expansion			
No.	Power, W	Θ_t	η	ζ	Θ_t	η	Error, %
1	2	0.924	0.773	0.211	0.920	0.804	4.0
2	2	0.934	0.801	0.175	0.931	0.829	3.5
3	4	0.888	0.723	0.375	0.878	0.714	1.2
4	4	0.904	0.776	0.311	0.893	0.745	4.0
5	10	0.810	0.599	0.861	0.799	0.560	6.5
6	10	0.830	0.637	0.690	0.821	0.603	5.3